

Relation Preserving Triplet Mining for Stabilizing the Triplet Loss in Vehicle Re-identification

Adhiraj Ghosh ^{* 1,2}, Kuruparan Shanmugalingam ^{†1,3}, and Wen-Yan Lin ^{‡1}

¹Singapore Management University, ²Zurich University of Applied Sciences, ³University of New South Wales

Abstract

Object appearances often change dramatically with pose variations. This creates a challenge for embedding schemes that seek to map instances with the same object ID to locations that are as close as possible. This issue becomes significantly heightened in complex computer vision tasks such as re-identification (re-id). In this paper, we suggest these dramatic appearance changes are indications that an object ID is composed of multiple natural groups and it is counter-productive to forcefully map instances from different groups to a common location. This leads us to introduce Relation Preserving Triplet Mining (RPTM), a feature matching guided triplet mining scheme, that ensures triplets will respect the natural sub-groupings within an object ID. We use this triplet mining mechanism to establish a pose-aware, well-conditioned triplet cost function. This allows a single network to be trained with fixed parameters across three challenging benchmarks, while still providing state-of-the-art re-identification results.

1. Introduction

Re-identification is the process of identifying images of the same object taken in different conditions. One of the main challenges of re-id is pose-induced appearance changes [1, 7]. Not only does object appearance change with pose, different objects often look similar when viewed from the same pose, also known as inverse-variability. This paper suggests a new interpretation of the inverse-variability problem, one with the potential to significantly improve the effectiveness of re-id algorithms. Although we focus on vehicle re-id, the underlying principles developed here are not restricted to this task and have the potential to

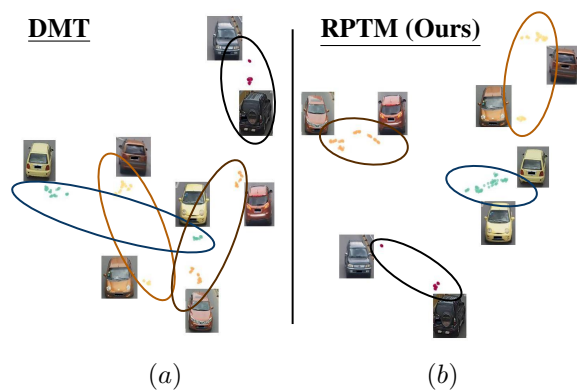


Figure 1: Comparing the features learned by DMT [14], a current state-of-the-art, with RPTM, our proposed Relation Preserving Triplet Mining. Features correspond to the first four IDs of Veri-776 [22, 23]. The distance preserving UMAP projection [27], shows the RPTM feature transform is more intuitive.

impact a wide range of computer vision problems.

Current re-identification frameworks attempt to learn embeddings that map semantically similar instances to relatively nearby locations; and semantically dissimilar images to relatively distant locations. This is typically achieved through a triplet loss function [36], which encourages a reference (anchor) input to be more similar to a positive (truthy) input than to a negative (falsy) input. The number of triplet combinations tend to grow polynomially with the number of instances in a dataset, as detailed by Hermans *et al.* [15]; however, most triplet combinations are redundant. This has led to the development of triplet mining, whose aim is to identify the most important triplets in a given set. While triplet mining is ubiquitous in re-identification algorithms [1, 14, 15, 32, 39], it has an innate vulnerability.

Consider a hypothetical dataset containing instances of

*ghos@zhaw.ch

†kuruparan@unsw.edu.au

‡daniellin@smu.edu.sg

apple-the-phone and apple-the-fruit, both of which are classified as Apple. The dataset also has instances of phones made by Samsung, which are classified as Samsung-phone. This dataset will have many difficult triplets, for example, apple-the-phone (anchor), apple-the-fruit (positive) and Samsung-phone (negative), which triplet-mining techniques will be encouraged to focus on. However, training with such triplets is counter-productive as they will attempt to ensure that instances of apple-the-phone are mapped closer to instances of apple-the-fruit than to instances of Samsung-phone. Such a mapping mechanism violates the natural appearance relation between objects and it is unlikely that models trained on this hypothesis will generalise in an adequate manner.

A similar phenomenon occurs in vehicle re-id. Most vehicular datasets [22, 23, 40] group instances by vehicle label or ID. However, the appearance of a vehicle’s front, rear and sides are often very different from each other because they belong to physically different entities. This creates the potential for fallacious anchor-positive pairs, where instances chosen to be anchor and positive do not share a natural group [1]. This problem has been acknowledged in recent re-identification works [7, 19, 28, 32, 39], who address it by incorporating pose awareness into the network. While this approach can be effective, it complicates network training and incurs an additional burden of training a new, dataset specific, pose-aware layer.

This paper suggests a simple alternative, where feature matching [3, 26] is leveraged to discover the natural groupings. The result is *Relation Preserving Triplet Mining* (RPTM), a triplet mining scheme which respects natural appearance groupings. In the context of vehicle re-identification, natural groupings tend to be pose-related. Here, RPTM implicitly enforces pose-aware triplet mining, which prevents different poses from being mapped onto one another. This improves the conditioning of the triplet-cost, allowing for the same training parameters to be employed across a variety of different datasets. The resultant feature embeddings provide better re-id results and are more intuitive, as shown in Figure 1.

In summary, our paper contributions are:

1. We explain that the traditional triplet mining methods are ill-conditioned because it does not take into account natural groupings;
2. We propose a feature guided triplet mining scheme that we term Relation Preserving Triplet Mining (RPTM);
3. We show RPTM is well-conditioned enough to permit the use of constant training parameters across three different datasets. The resultant network is simultaneously capable of state-of-the-art in vehicle re-id and competitive results for person re-id.

2. Related Works

Re-Identification: The demand for urban surveillance applications has led to a surge of interest in person and vehicle re-identification. Challenging benchmarks like VehicleID [21], Veri-776 [22, 23], DukeMTMC [34], CityFlow [40], VERI-Wild [24], Market-1501 [50] and others have been established; and many new algorithms have been proposed [7, 13, 14, 18, 19, 24, 28, 39, 53]. Most works use a combination of a classification loss and ranking loss such as Triplet loss. However, new methods employing Circle loss [38], Center loss [43], Angular Margin loss [8] and others have shown promising results.

This paper primarily focuses on vehicle re-identification. As mentioned in the introduction, many vehicle re-id algorithms achieve good results by estimating vehicular pose. Towards this end, Zhou and Shao [53] used GANs to generate multiple new views from a single vehicular image, Tang *et al.* [39] created a synthetic dataset to implement vehicle pose-estimation, and Meng *et al.* [28] used a parser network to split vehicles into four parts to achieve pose-aware feature embedding. Apart from the pose-based techniques, there also are a wide variety of vehicle re-identification algorithms that employ "exotic" techniques to advance the state-of-the-art. Examples include expanded training by combining past datasets [51], and integrated local and global constraints through detection branches [13].

We suggest that the root-problem encountered by most of these techniques lies in their triplet loss definition. By replacing traditional triplet losses with our RPTM technique, we show that it is possible to achieve state-of-the-art results by minimizing a simple cost function. This stands out from the trend towards ever more complex vehicle re-id techniques.

Triplet Loss: The triplet loss was first introduced in the context of face re-identification [36]. Since then, it has undergone many refinements [1, 37, 45, 46, 48] and been applied to a wide range of applications, such as, object tracking [9], object retrieval and face verification [10].

Such triplet-based formulations implicitly assume that the given IDs correspond to meaningful groups. We suggest that this assumption is often wrong and that triplets should be defined with respect to naturally occurring groups rather than the given labels.

This perspective on triplet loss differs significantly from that used in most papers. To our knowledge, the research most similar to ours is Bai *et al.* [1]. Like us, Bai *et al.* acknowledges the importance of naturally occurring groups within an ID. However, Bai *et al.* attempts to use the groups to force tighter mappings of an ID, fighting rather than harnessing the natural relationships.

Another problem for clustering based works like Bai *et al.* [1]’s, is that variations often have no naturally occurring cluster boundaries. This is not a problem for RPTM which

defines relations in a pairwise manner, rather than on the basis of shared clusters.

Feature Matching: RPTM uses feature matching to help establish triplets. Feature matching is a well-established field in computer vision whose goal is to match key-points between image pairs. Classic feature matching works include SIFT [26], SURF [2], ASIFT [29], ORB [35], LIFT [47], *etc.* In this paper, we employ Grid-based Motion Statistics (GMS) [3] as our feature matcher of choice. This is a newer algorithm which incorporates match coherence [20] to facilitate key-point matching. GMS outperforms most classic techniques while also being much faster.

3. Why Triplet Loss? From Classification to Re-identification

This section explains the machine learning trends which led to the development of the triplet loss.

3.1. Neural Networks as Embedding Functions

Much of computer vision can be interpreted as an attempt to map image instances to a semantically meaningful embedding. Thus, if \mathbf{x}_k represents an image instance and \mathbf{y}_k its associated feature, the transformation from \mathbf{x}_k to \mathbf{y}_k can be denoted by:

$$\mathbf{y}_k = f(\mathbf{x}_k), \quad (1)$$

where $f : \mathbb{R}^{3 \times w \times h} \rightarrow \mathbb{R}^d$; $w \times h$ denotes image dimension; and d represents the embedding space's dimensions.

Deep-learners often estimate the embedding indirectly through a cross-entropy minimization. This takes the form of a loss function

$$\mathcal{L}_{ent}(\mathbf{x}_k) = -\frac{1}{n} \sum_{i=1}^n l_i \cdot \log(\hat{l}_i), \quad (2)$$

where $l_{ik} \in \{0, 1\}$ is a binary indicator of whether instance k is a member of class i ; \mathbf{w}_j, b_j represent the weights and bias of the deep-learner's soft-max layer; and

$$\hat{l}_{ik} = \frac{e^{\mathbf{y}_k \cdot \mathbf{w}_i + b_i}}{\sum_{j=1}^N e^{\mathbf{y}_k \cdot \mathbf{w}_j + b_j}}$$

is the soft-max's estimation of l_{ik} .

In this scheme, the embedding function $f(\cdot)$ is learned by minimizing the cross-entropy loss

$$E_{ent} = \sum_{k=1}^m \mathcal{L}_{ent}(\mathbf{x}_k), \quad (3)$$

where m denotes the total number of training images.

Minimizing the cost in Eq. 3 provides an embedding that maximizes classification accuracy. However, this does

not ensure the embedding is semantically meaningful. The retrieval problem requires an embedding in which semantically similar instances are mapped close to one another, giving rise to the development of the triplet loss [36].

3.2. The Triplet Loss

A triplet loss is defined with respect to three image instances: Anchor (a randomly chosen instance); Positive (an instance that shares a common ID with the anchor); Negative (an instance whose ID is different from the anchor). We denote these instances $\mathbf{x}_a, \mathbf{x}_p$ and \mathbf{x}_n respectively.

Given the anchor, positive and negative, the triplet loss is defined as [36]:

$$\mathcal{L}_{tri}(\mathbf{x}_a, \mathbf{x}_p, \mathbf{x}_n) = \max(0, d_{ap} - d_{an} + \alpha), \quad (4)$$

where α is the desired margin separation between the positive and negative instance, $d_{ap} = \|f(\mathbf{x}_a) - f(\mathbf{x}_p)\|$ and $d_{an} = \|f(\mathbf{x}_a) - f(\mathbf{x}_n)\|$.

The final triplet-cost is computed by summing the individual triplet losses:

$$E_{tri} = \sum_{c=1}^t \mathcal{L}_{tri}(\mathbf{x}_{ac}, \mathbf{x}_{pc}, \mathbf{x}_{nc}), \quad (5)$$

where t is the total number of triplets.

In general, triplet-costs are not used in isolation. Instead, they are combined with the cross-entropy-cost from Eq. 3, leading to the final cost function:

$$E = \lambda_{ent} E_{ent} + \lambda_{tri} E_{tri}, \quad (6)$$

where λ_{ent} and λ_{tri} control the weights given to the cross-entropy loss and triplet-cost respectively.

4. Relation Preserving Triplet Mining

Naïvely incorporating every possible triplet into the triplet-cost usually yields poor results [15]. Instead, training algorithms employ triplet-mining, a process which aims to incorporate only the most relevant triplets into the triplet-cost. Unfortunately, there is no consensus regarding how relevance can be measured; thus, triplet-mining relies on heuristics. The two most popular heuristics are: hard-negative mining and semi-hard negative mining.

Hard-negative mining focuses on triplets whose negatives are very similar to the anchor. Semi-hard negative mining shifts the focus from the hardest negatives, to negatives close to the decision boundary. Both heuristics seem sensible and often perform well; however, closer inspection suggests something may be amiss.

Let us perform a thought experiment where we assign the IDs A and B, to similar car models. Hard or semi-hard negative mining will find the most confusing triplets, leading to the following triplet: front of car A as anchor, rear of car

A as positive, and front of car B as negative. The triplet is indeed very hard; however, its incorporation into the training cost is counter-productive. This is because such a triplet encourages an embedding which maps the rear of car A to the front of car A. The embedding is so counter-intuitive, it is unlikely to generalise well. To avoid such pathological cases, we introduce relational triplets, which addresses the problem of intra-class separability with greater attention than other triplet mining methods.

4.1. Relational Triplets

Relational triplets change the triplet definition from one based on human assigned IDs to one based on naturally occurring groups. Formally, we denote the set of training images as:

$$\mathcal{S} = \{\mathbf{x}_1, \mathbf{x}_2, \dots, \mathbf{x}_K\}.$$

We hypothesize that these images are members of naturally occurring (and possibly overlapping) subsets. The set of subsets is denoted by:

$$\mathcal{N} = \{\mathcal{S}_m\},$$

where

$$\mathcal{S} = \bigcup_{\mathcal{S}_m \in \mathcal{N}} \mathcal{S}_m. \quad (7)$$

We use the relational indicator

$$C(\mathbf{x}_i, \mathbf{x}_j) = \begin{cases} 1, & \text{if } \mathbf{x}_i, \mathbf{x}_j \text{ share a subset in } \mathcal{N}, \\ 0, & \text{otherwise.} \end{cases} \quad (8)$$

to denote whether two instances share a natural subset.

A relational triplet is one where the anchor-positive pair shares a common natural subset, while the negative does not. *i.e.*

$$C(\mathbf{x}_a, \mathbf{x}_p) = 1, \quad C(\mathbf{x}_a, \mathbf{x}_n) = 0, \quad C(\mathbf{x}_p, \mathbf{x}_n) = 0. \quad (9)$$

Traditional triplets are a special case of relational triplets, where the given IDs mirror the natural subsets. This is not the case for vehicular re-identification, as we explained in the thought experiment and through the relational diagram in Figure 2.

In vehicle re-id, the natural subsets likely correspond to vehicular poses. This creates the possibility for identifying such subsets using a feature matching algorithm. The next section shows how this can be achieved.

4.2. Mining the Relation Preserving Triplets

GMS [3] is a modern feature matcher that uses coherence to validate hypothesized feature matches. The coherence scheme assumes that a true match hypothesis will be strongly supported by many other match hypotheses between neighbouring region pairs, while a false match hypothesis will not have such support.

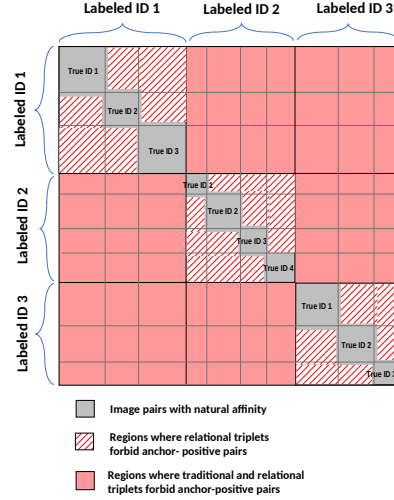


Figure 2: Affinity matrix for vehicular images. Each vehicular ID contains a number of naturally occurring groups. Pathological triplets arise when anchor-positive pairs do not have natural affinity (share a common group). Observe that the traditional ID based triplet permits pathological anchor-positive pairs. Relational triplets are based on natural groups rather than IDs, thus preventing pathological anchor-positives.

The coherence-based validation is notably better than the traditional ratio test [26]. This allows GMS to reliably match features across significant viewpoint changes, while simultaneously ensuring few matches between image pairs with nothing in common. As a result, the presence of GMS matches between image pairs provides a good approximation of the relational indicator in Eq. 7.

While GMS has few errors, errors do occur. To ensure an anchor-positive pair has a relational indicator of one, we set the positive instance of each anchor to be the image instance, whose number of GMS matches with the anchor is closest to the threshold τ . At this junction, we accept that setting similar anchor-positive pairs lead to poorer training. Hence, we use a middle-ground approach for anchor-positive selection, which we call $RPTM_{mean}$, in which τ is set as the average number of GMS matches in the set of non-zero pairwise GMS matches between the anchor and all other images.

The above provides a semi-hard positive mining, that ensures anchor-positive pairs satisfy the relational indicator in Eq. 7, while also ensuring the positive differs significantly from the anchor. An example is shown in Figure 3.

We define negatives using batch-hard-triplet mining [15]. If $\mathcal{S}_b = \{\mathbf{x}_j\}$ denotes the set of instances in a

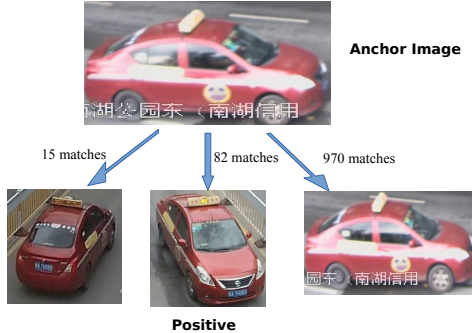


Figure 3: An example of the anchor-positive pairs selected by relation preserving triplet mining. Observe that the positive shares clear similarities with the anchor (indicating they share a common natural group) but is not a near-duplicate.

batch that do not share an ID with \mathbf{x}_a , the negative is

$$\mathbf{x}_n = \operatorname{argmin}_{\mathbf{x}_j \in S_b} (\|f(\mathbf{x}_a) - f(\mathbf{x}_j)\|). \quad (10)$$

Observe that the triplets defined in this manner satisfy Eq. 9, making them relation preserving triplets. Given such triplets, the final embedding can be obtained by minimising the cost function in Eq. 6. As evidenced by the mining strategy, RPTM allows for the intrinsic understanding of viewpoint and pose without hard-coded pose estimation.

5. Implementation Details

A schematic for the network architecture is provided in Figure 4. In this section we discuss the model layout, elaborating on the comparative feature matching pipeline in Section 5.1 and the SE-ResNext101-ibn model structure with RPTM in Section 5.2. To test and highlight the universality of RPTM and its ability to generalise the training pipeline due to its novel triplet mining scheme, we put limitations on network and parameter tuning across all datasets.

5.1. Feature Matching

As discussed in the earlier sections, we use GMS feature matching to guide our triplet-mining process, in order to implement semi-hard positive mining during. In theory, we need to establish GMS matches between an anchor and every other image in the dataset. In practice, we use image IDs as guides to the natural groupings and restrict matching to only images sharing a common ID with the anchor. This greatly reduces computational cost in triplet mining.

Feature matching is performed on images that have been resized to (224, 224). The GMS feature matching parameters are: 10,000 ORB features [35] whose orientation parameter is set to true and nearest neighbours are identified

with the brute-force hamming distance. All other parameters are set based on the reported guidelines of [3]. After matching, the number of matches between image pairs is stored in an $m \times m$ relational matrix, where m is the number of training images.

5.2. Neural Network

Our base network is ResNext101, appended with instance-batch-normalization [31] and a squeeze-excitation layer [16]. The weights of this network are trained by minimising the combined cross-entropy and triplet loss in Eq. 6. Triplet selection is performed using the precomputed GMS features and the Relation Preserving Triplet Mining described in Section. 4.2.

For vehicle re-id, images are resized to (240,240); while for person re-id, images are resized to (300,150). Data augmentation is applied, with random flipping, random padding, random erasing and colour jitter (randomly changing contrast, brightness, hue and saturation) all activated. Stochastic Gradient Descent(SGD) is used as the optimizer for the model. The initial learning rate is initialized at 0.005 and is set to decay by a factor of 0.1 every 20 epochs. The model is trained for 80 epochs with a batch size of 24. The training parameters are fixed for all datasets.¹

6. Experiments

Our backbone network is created by appending an instance-batch-normalization (IBN [31]) and squeeze-excitation layer (SE [16]) to a ResNext101 model. This network is trained using triplets defined through our Relation Preserving Triplet Mining (RPTM). The network is denoted SE-ResNext101-ibn (RPTM) or RPTM for short.

6.1. Datasets

Veri-776 [22] is a widely used benchmark with a diverse range of viewpoints for each vehicle. The dataset contains 51,027 images from 776 distinct vehicles and is designed to provide more constrained but highly realistic conditions.

VehicleID [21] contains 221,567 images of 26,328 distinct vehicles. This dataset allows us to test RPTM’s scalability by offering multiple, progressively larger (and harder) test-sets. We evaluate our algorithm on small, medium and large test sets, with 800, 1600 and 2400 labels for testing.

DukeMTMC [34] is a person re-identification benchmark with 36,411 images and 1,404 distinct people. While our focus is vehicle re-id, we include this benchmark to show our algorithm can generalise to other problems.

6.2. Evaluation Metrics

Algorithms are evaluated on a set of query and gallery images. Each algorithm is tasked with transforming the im-

¹These parameters are significantly less computationally demanding than those used by recent state-of-the-art models [7, 14, 18, 51, 53].

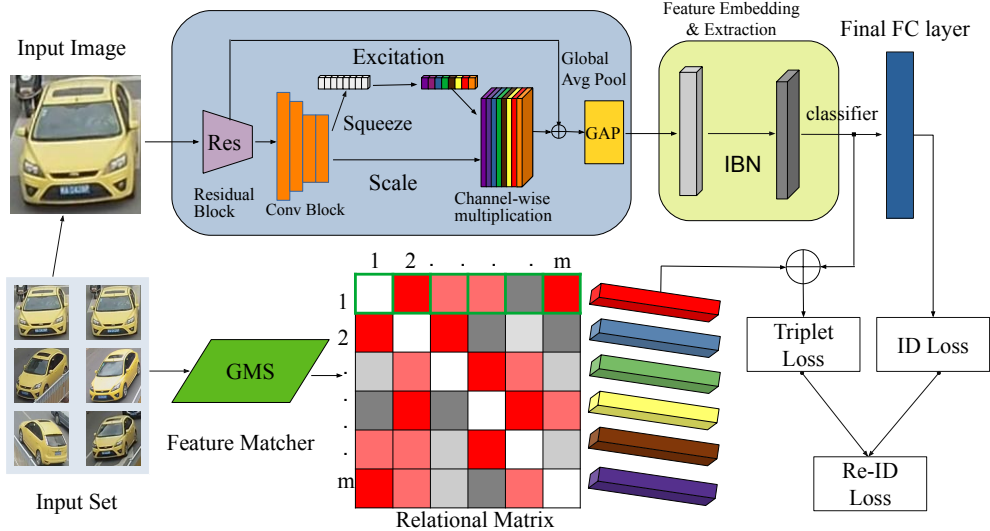


Figure 4: Schematic of a re-identification network deploying **Relation Preserving Triplet Mining**. The backbone network is appended with Instance-Batch Normalisation (IBN) and Squeeze-Excitation (SE) to boost performance and reduce channel inter-dependencies. The relational matrix is estimated using GMS matches and is used for triplet selection.

ages into feature vectors. For a given query feature, the gallery features are ranked by their Euclidean distance from it. The ranking is then scored, with an ideal ranking being one in which all gallery features sharing an ID with the query, are ranked highest.

Rankings are scored according to the protocols suggested in [21, 23]. Thus, we report three results: mean average precision (mAP); Cumulative Matching Characteristics at top-1 (rank-1) and Cumulative Matching Characteristics at top-5 (rank-5). Mean average precision provides an overall gauge of the ranking’s accuracy, while rank-1 and rank-5 measure how often a correct ID is present within the top-1 and top-5 ranked gallery images.

Following the conventions for the Veri-776 and DukeMTMC dataset, we use the re-ranking methodology proposed in [52]. This post-processor refines the final rankings by considering the k-reciprocal nearest-neighbours of both the query and retrieved images, effectively improving upon the pairwise distance result that is used to quantify mAP and top-k ranking accuracies. Re-ranking is not adopted for VehicleID because there is often only one true match ID in the gallery set [18].

6.3. Comparison with State-of-the-art

Veri-776: As shown in table 1, RPTM surpasses recent state-of-the-art vehicle re-id models. These results are very respectable, especially if we account for the fact that the next best algorithm (by mAP), VehicleNet [51] uses supplementary data for training. We also edge out DMT [14]

Model	mAP	r = 1	r = 5
GSTE [1]	59.47	96.24	98.97
VANet [7]	66.34	89.78	95.99
SPAN [5]	68.90	94.00	97.60
PAMTRI [39]	71.88	92.86	96.97
PVEN [28]	79.50	95.60	98.40
RPTM(Ours)	80.60	95.90	98.50
GAN+LSRO* [44]	64.78	88.62	94.52
AAVER* [18]	66.35	90.17	94.34
SAVER* [19]	82.00	96.90	97.70
DMT* [14]	82.00	96.90	–
VehicleNet* [51]	83.41	96.78	–
RPTM(Ours)*	87.40	96.20	98.10

Table 1: Comparison with the State-of-the-art results on the Veri-776 dataset. Our RPTM algorithm is able to set the state-of-the-art in mAP and produces comparable results in rank-1 and rank-5 accuracies too. The * indicates the usage of re-ranking in evaluation.

in mAP results, which uses deeper backbones and larger image sizes during training. In addition, RPTM’s training scheme is very simple, as it only requires gradient descent on a well-defined cost-function.

VehicleID: Table 2 shows that RPTM achieves state-of-the-art results on the challenging VehicleID dataset, indicating RPTM’s scalability across vehicle datasets. We observe

Model	Small (query size=800)			Medium (query size=1600)			Large (query size=2400)		
	mAP	r=1	r=5	mAP	r=1	r=5	mAP	r=1	r=5
VAMI [53]	-	63.12	83.25	-	52.87	75.12	-	47.34	70.29
C2F-Rank [11]	63.50	61.10	81.70	60.00	56.20	76.20	53.00	51.40	72.20
DenseNet121 [17]	68.85	66.10	77.87	69.45	67.39	75.49	65.37	63.07	72.57
AAVER [18]	-	74.69	93.82	-	68.62	89.95	-	63.54	85.64
AGNet [49]	76.06	73.14	86.25	73.39	70.77	81.75	71.75	69.10	80.40
QD-DLP [54]	76.54	72.32	92.48	74.63	70.66	88.90	68.41	64.14	83.37
Hard-View-EALN [25]	77.50	75.11	88.09	74.20	71.78	83.94	71.00	69.30	81.42
VehicleNet [51]	-	83.64	96.86	-	81.35	93.61	-	79.46	92.04
VANet [7]	-	88.12	97.29	-	83.10	95.14	-	80.35	92.97
Smooth-AP [4]	-	94.90	97.60	-	93.30	96.40	-	91.90	96.20
RPTM	84.80	95.10	97.40	81.20	93.30	96.90	80.50	92.70	96.50

Table 2: Comparison on VehicleID. RPTM provides the state-of-the-art retrieval on all three test sets, with notably better performance on the most difficult, large test set.

RPTM out-performing VANet [7] comprehensively across all recall metrics. Additionally, RPTM exceeds Smooth-AP[4] in 4 of 6 metrics, notably in the large test-set.

DukeMTMC: Table 3 shows RPTM achieves competitive results at person re-identification, despite training parameters tuned to vehicle datasets. With the exception of changing the input image size, to account for the aspect ratio of the input images, no modification were made to RPTM’s network or training parameters. These results are very respectable for a network whose training parameters are tuned for a different task.

Discussion: Table 1, 2 and 3, show that incorporating RPTM to feature learning techniques make them more effective at re-identification. Performance improvements are especially notable on more difficult datasets like VehicleID and harsher evaluation metrics (mAP). These performances are rather remarkable when we take into account that RPTM uses constant training parameters for all three datasets. Most deep-learning algorithms require parameters to be tweaked from dataset to dataset and RPTM’s capability in this respect is an indication that relational aware triplet choice makes the triplet-losses better conditioned.

To demonstrate how challenging it is to maintain constant training parameters, we trained Smooth-AP [4] from Table 2 on two other datasets, while using the training parameters from Table 2. Although Smooth-AP [4] is comparable to RPTM in Table 2 on VehicleID, its is much inferior on the other datasets shown in Table 4.

6.4. Ablation Study

Image Size: We begin by investigating how image size impacts re-identification. Table 5 shows accuracy improves as image size increases, a finding that is mirrored by many other re-id algorithms, which often seek to use the largest possible image.

Model	mAP	r = 1	r = 5
P2-Net [12]	73.1	86.5	93.1
SCSN [6]	79.0	91.0	-
GPS [30]	78.7	88.2	95.2
RPTM(Ours)	77.9	87.8	96.0
PFSAN* [42]	85.9	89.0	-
Top-DB-Net* [33]	88.6	90.9	-
st-reID* [41]	92.7	94.5	96.8
RPTM(Ours)*	86.2	90.6	95.4

Table 3: Comparison on the DukeMTMC benchmark. RPTM is surprisingly competitive even though it is not tuned for maximum accuracy in person re-identification. * indicates the use of re-ranking.

	mAP	r = 1	r = 5
Smooth-AP (Veri-776)	72.40	91.10	94.20
RPTM (Veri-776)	87.40	96.20	98.10
Smooth-AP (DukeMTMC)	65.70	79.90	88.40
RPTM (DukeMTMC)	86.20	90.60	95.40

Table 4: Performance of Smooth-AP [4] on Veri-776 and DukeMTMC. Results include re-ranking as a post-processing step.

Threshold for Positive Selection: Section 4.2 suggests positive images are chosen using a threshold, τ , which is the mean number of non-zero matching results. We denote this scheme $RPTM_{mean}$; it corresponds to semi-hard positive mining. There are a number of alternatives.

One possibility is to fix τ at a low number of matches, like 10. We term this scheme $RPTM_{min}$. The scheme ensures anchor-positive pairs are not near duplicates and cor-

Model	Veri-776		VehicleID(Small)	
	mAP	r=1	mAP	r=1
$RPTM_{128 \times 128}$	56.5	84.5	72.5	89.0
$RPTM_{160 \times 160}$	74.8	92.4	80.5	91.8
$RPTM_{224 \times 224}$	85.1	95.2	83.1	92.9
$RPTM_{240 \times 240}$	87.4	96.2	84.8	95.1

Table 5: Re-identification performance with increasing image size. mAP and rank-1 increase with image size until (240, 240), after which performance plateaus.

responds to hard positive mining. The drawback is a vulnerability to occasional matching errors.

Another possibility is to set τ to the largest number of matches an anchor image has. We term this $RPTM_{max}$. This eliminates any vulnerability to GMS matching errors but sacrifices the positive image’s distinctiveness. This corresponds to easy positive mining. Table 6 indicates $RPTM_{mean}$ has the best performance; thus, it is adopted as the default scheme for positive image mining.

Model	mAP	r = 1	r = 5
$RPTM_{min}$	86.3	95.9	97.2
$RPTM_{mean}$ (our default)	87.4	96.2	98.1
$RPTM_{max}$	82.2	95.6	97.4

Table 6: Comparing positive selection thresholds. $RPTM_{min}$ corresponds to hard positive-mining, $RPTM_{mean}$ corresponds to semi-hard positive-mining, $RPTM_{max}$ corresponds to easy positive-mining.

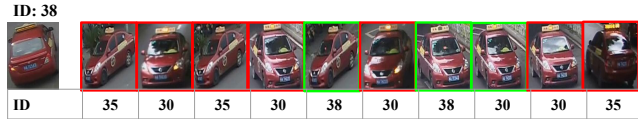
Veri-776			
Model	mAP	r = 1	r = 5
ResNet50	65.0	88.1	93.7
ResNet50 (RPTM)	81.7	94.2	96.4
ResNet101	65.6	87.6	94.5
ResNet101(RPTM)	82.8	95.4	97.1
ResNet101-ibn	71.5	94.2	96.9
ResNet101-ibn (RPTM)	83.3	95.6	97.5
SE-ResNext101-ibn	81.3	93.5	96.8
SE-ResNext101-ibn (RPTM)	87.4	96.2	98.1

Table 7: RPTM consistently improves the underlying network. Improvements are especially large for simple networks like ResNet50.

Network Ablation: To understand the impact of each component, we progressively upgrade a basic ResNet until it reaches the full SE-ResNext101-ibn. At each stage, performance with and without RPTM is compared; results are presented in Table 7. Table 7 shows that at each stage,



(a) Top: Retrieval results with SE-ResNext101-ibn. Bottom: Retrieval results with SE-ResNext101-ibn (RPTM).



(b) Top: Retrieval results with SE-ResNext101-ibn. Bottom: Retrieval results with SE-ResNext101-ibn (RPTM).

Figure 5: Re-identification on Veri-776. Correct identifications are outlined in green; wrong ones are outlined in red. RPTM helps SE-ResNext101-ibn avoid many errors.

RPTM consistently improves the re-id performance of the underlying backbone network. The gains being especially notable for simpler networks like ResNet50. These gains are so high that ResNet50 (RPTM)’s performance almost matches the more sophisticated SE-ResNext101-ibn, without RPTM. Finally, Figure 5 provides qualitative comparisons which shows RPTM’s top-k ranked retrievals are significantly better than its backbone network.

7. Conclusion

This paper suggests triplet mining needs to respect natural data groupings. To that end, we introduce Relation Preserving Triplet Mining (RPTM), a novel scheme to generate triplets that are wary of the inverse-variability problem, which deeply affect re-id pipelines. We show how feature matches can be used to develop a relation aware triplet mining, leading to a better conditioned triplet loss. This allows feature learners with enhanced training stability and higher re-identification accuracy. Moreover, we highlight that not only does RPTM outperform recent vehicle re-identification models while maintaining constant training parameters across datasets, but it also reproduces highly competitive results for person re-identification, with the same training parameters.

References

- [1] Yan Bai, Yihang Lou, Feng Gao, Shiqi Wang, Yuwei Wu, and Ling-Yu Duan. Group-sensitive triplet embedding for vehicle reidentification. *IEEE Transactions on Multimedia*, 20(9):2385–2399, 2018.
- [2] Herbert Bay, Tinne Tuytelaars, and Luc Van Gool. Surf: Speeded up robust features. In *European conference on computer vision*, pages 404–417. Springer, 2006.
- [3] JiaWang Bian, Wen-Yan Lin, Yasuyuki Matsushita, Sai-Kit Yeung, Tan-Dat Nguyen, and Ming-Ming Cheng. Gms: Grid-based motion statistics for fast, ultra-robust feature correspondence. In *Proceedings of the IEEE conference on computer vision and pattern recognition*, pages 4181–4190, 2017.
- [4] Andrew Brown, Weidi Xie, Vicky Kalogeiton, and Andrew Zisserman. Smooth-ap: Smoothing the path towards large-scale image retrieval. In *European Conference on Computer Vision*, pages 677–694. Springer, 2020.
- [5] Tsai-Shien Chen, Chih-Ting Liu, Chih-Wei Wu, and Shao-Yi Chien. Orientation-aware vehicle re-identification with semantics-guided part attention network. In *European Conference on Computer Vision*, pages 330–346. Springer, 2020.
- [6] Xuesong Chen, Canmiao Fu, Yong Zhao, Feng Zheng, Jingkuan Song, Rongrong Ji, and Yi Yang. Saliency-guided cascaded suppression network for person re-identification. In *Proceedings of the IEEE/CVF Conference on Computer Vision and Pattern Recognition*, pages 3300–3310, 2020.
- [7] Ruihang Chu, Yifan Sun, Yadong Li, Zheng Liu, Chi Zhang, and Yichen Wei. Vehicle re-identification with viewpoint-aware metric learning. In *Proceedings of the IEEE/CVF International Conference on Computer Vision*, pages 8282–8291, 2019.
- [8] Jiankang Deng, Jia Guo, Niannan Xue, and Stefanos Zafeiriou. Arcface: Additive angular margin loss for deep face recognition. In *Proceedings of the IEEE/CVF Conference on Computer Vision and Pattern Recognition*, pages 4690–4699, 2019.
- [9] Xingping Dong and Jianbing Shen. Triplet loss in siamese network for object tracking. In *Proceedings of the European conference on computer vision (ECCV)*, pages 459–474, 2018.
- [10] Weifeng Ge. Deep metric learning with hierarchical triplet loss. In *Proceedings of the European Conference on Computer Vision (ECCV)*, pages 269–285, 2018.
- [11] Haiyun Guo, Chaoyang Zhao, Zhiwei Liu, Jinqiao Wang, and Hanqing Lu. Learning coarse-to-fine structured feature embedding for vehicle re-identification. In *Proceedings of the AAAI Conference on Artificial Intelligence*, volume 32, 2018.
- [12] Jianyuan Guo, Yuhui Yuan, Lang Huang, Chao Zhang, Jin-Ge Yao, and Kai Han. Beyond human parts: Dual part-aligned representations for person re-identification. In *Proceedings of the IEEE/CVF International Conference on Computer Vision*, pages 3642–3651, 2019.
- [13] Bing He, Jia Li, Yifan Zhao, and Yonghong Tian. Part-regularized near-duplicate vehicle re-identification. In *Proceedings of the IEEE/CVF Conference on Computer Vision and Pattern Recognition*, pages 3997–4005, 2019.
- [14] Shuting He, Hao Luo, Weihua Chen, Miao Zhang, Yuqi Zhang, Fan Wang, Hao Li, and Wei Jiang. Multi-domain learning and identity mining for vehicle re-identification. In *Proceedings of the IEEE/CVF Conference on Computer Vision and Pattern Recognition Workshops*, pages 582–583, 2020.
- [15] Alexander Hermans, Lucas Beyer, and Bastian Leibe. In defense of the triplet loss for person re-identification. *arXiv preprint arXiv:1703.07737*, 2017.
- [16] Jie Hu, Li Shen, and Gang Sun. Squeeze-and-excitation networks. In *Proceedings of the IEEE conference on computer vision and pattern recognition*, pages 7132–7141, 2018.
- [17] Gao Huang, Zhuang Liu, Laurens Van Der Maaten, and Kilian Q Weinberger. Densely connected convolutional networks. In *Proceedings of the IEEE conference on computer vision and pattern recognition*, pages 4700–4708, 2017.
- [18] Pirazh Khorramshahi, Amit Kumar, Neehar Peri, Sai Saketh Rambhatla, Jun-Cheng Chen, and Rama Chellappa. A dual-path model with adaptive attention for vehicle re-identification. In *Proceedings of the IEEE/CVF International Conference on Computer Vision*, pages 6132–6141, 2019.
- [19] Pirazh Khorramshahi, Neehar Peri, Jun-cheng Chen, and Rama Chellappa. The devil is in the details: Self-supervised attention for vehicle re-identification. In *European Conference on Computer Vision*, pages 369–386. Springer, 2020.
- [20] Wen-Yan Daniel Lin, Ming-Ming Cheng, Jiangbo Lu, Hongsheng Yang, Minh N Do, and Philip Torr. Bilateral functions for global motion modeling. In *European Conference on Computer Vision*, pages 341–356. Springer, 2014.
- [21] Hongye Liu, Yonghong Tian, Yaowei Wang, Lu Pang, and Tiejun Huang. Deep relative distance learning: Tell the difference between similar vehicles. In *Proceedings of the IEEE Conference on Computer Vision and Pattern Recognition*, pages 2167–2175, 2016.
- [22] Xinchun Liu, Wu Liu, Huadong Ma, and Huiyuan Fu. Large-scale vehicle re-identification in urban surveillance videos. In *2016 IEEE International Conference on Multimedia and Expo (ICME)*, pages 1–6. IEEE, 2016.
- [23] Xinchun Liu, Wu Liu, Tao Mei, and Huadong Ma. A deep learning-based approach to progressive vehicle re-identification for urban surveillance. In *European conference on computer vision*, pages 869–884. Springer, 2016.
- [24] Yihang Lou, Yan Bai, Jun Liu, Shiqi Wang, and Lingyu Duan. Veri-wild: A large dataset and a new method for vehicle re-identification in the wild. In *Proceedings of the IEEE/CVF Conference on Computer Vision and Pattern Recognition*, pages 3235–3243, 2019.
- [25] Yihang Lou, Yan Bai, Jun Liu, Shiqi Wang, and Ling-Yu Duan. Embedding adversarial learning for vehicle re-identification. *IEEE Transactions on Image Processing*, 28(8):3794–3807, 2019.
- [26] David G Lowe. Object recognition from local scale-invariant features. In *Proceedings of the seventh IEEE international conference on computer vision*, volume 2, pages 1150–1157. Ieee, 1999.

- [27] Leland McInnes, John Healy, Nathaniel Saul, and Lukas Großberger. Umap: Uniform manifold approximation and projection. *Journal of Open Source Software*, 3(29):861, 2018.
- [28] Dechao Meng, Liang Li, Xuejing Liu, Yadong Li, Shijie Yang, Zheng-Jun Zha, Xingyu Gao, Shuhui Wang, and Qingming Huang. Parsing-based view-aware embedding network for vehicle re-identification. In *Proceedings of the IEEE/CVF Conference on Computer Vision and Pattern Recognition*, pages 7103–7112, 2020.
- [29] Jean-Michel Morel and Guoshen Yu. Asift: A new framework for fully affine invariant image comparison. *SIAM journal on imaging sciences*, 2(2):438–469, 2009.
- [30] Binh X Nguyen, Binh D Nguyen, Tuong Do, Erman Tjiputra, Quang D Tran, and Anh Nguyen. Graph-based person signature for person re-identifications. In *Proceedings of the IEEE/CVF Conference on Computer Vision and Pattern Recognition*, pages 3492–3501, 2021.
- [31] Xingang Pan, Ping Luo, Jianping Shi, and Xiaoou Tang. Two at once: Enhancing learning and generalization capacities via ibn-net. In *Proceedings of the European Conference on Computer Vision (ECCV)*, pages 464–479, 2018.
- [32] Angelo Porrello, Luca Bergamini, and Simone Calderara. Robust re-identification by multiple views knowledge distillation. In *European Conference on Computer Vision*, pages 93–110. Springer, 2020.
- [33] Rodolfo Quispe and Helio Pedrini. Top-db-net: Top drop-block for activation enhancement in person re-identification. *arXiv preprint arXiv:2010.05435*, 2020.
- [34] Ergys Ristani, Francesco Solera, Roger Zou, Rita Cucchiara, and Carlo Tomasi. Performance measures and a data set for multi-target, multi-camera tracking. In *European conference on computer vision*, pages 17–35. Springer, 2016.
- [35] Ethan Rublee, Vincent Rabaud, Kurt Konolige, and Gary Bradski. Orb: An efficient alternative to sift or surf. In *2011 International conference on computer vision*, pages 2564–2571. Ieee, 2011.
- [36] Florian Schroff, Dmitry Kalenichenko, and James Philbin. Facenet: A unified embedding for face recognition and clustering. In *Proceedings of the IEEE conference on computer vision and pattern recognition*, pages 815–823, 2015.
- [37] Hailin Shi, Yang Yang, Xiangyu Zhu, Shengcai Liao, Zhen Lei, Weishi Zheng, and Stan Z Li. Embedding deep metric for person re-identification: A study against large variations. In *European conference on computer vision*, pages 732–748. Springer, 2016.
- [38] Yifan Sun, Changmao Cheng, Yuhan Zhang, Chi Zhang, Liang Zheng, Zhongdao Wang, and Yichen Wei. Circle loss: A unified perspective of pair similarity optimization. In *Proceedings of the IEEE/CVF Conference on Computer Vision and Pattern Recognition*, pages 6398–6407, 2020.
- [39] Zheng Tang, Milind Naphade, Stan Birchfield, Jonathan Tremblay, William Hodge, Ratnesh Kumar, Shuo Wang, and Xiaodong Yang. Pamtri: Pose-aware multi-task learning for vehicle re-identification using highly randomized synthetic data. In *Proceedings of the IEEE International Conference on Computer Vision*, pages 211–220, 2019.
- [40] Zheng Tang, Milind Naphade, Ming-Yu Liu, Xiaodong Yang, Stan Birchfield, Shuo Wang, Ratnesh Kumar, David Anastasiu, and Jenq-Neng Hwang. Cityflow: A city-scale benchmark for multi-target multi-camera vehicle tracking and re-identification. In *Proceedings of the IEEE/CVF Conference on Computer Vision and Pattern Recognition*, pages 8797–8806, 2019.
- [41] Guangcong Wang, Jianhuang Lai, Peigen Huang, and Xiaohua Xie. Spatial-temporal person re-identification. In *Proceedings of the AAAI conference on artificial intelligence*, volume 33, pages 8933–8940, 2019.
- [42] Haoran Wang, Yue Fan, Zexin Wang, Licheng Jiao, and Bernt Schiele. Parameter-free spatial attention network for person re-identification. *arXiv preprint arXiv:1811.12150*, 2018.
- [43] Yandong Wen, Kaipeng Zhang, Zhifeng Li, and Yu Qiao. A discriminative feature learning approach for deep face recognition. In *European conference on computer vision*, pages 499–515. Springer, 2016.
- [44] Fangyu Wu, Shiyang Yan, Jeremy S Smith, and Bailing Zhang. Joint semi-supervised learning and re-ranking for vehicle re-identification. In *2018 24th International Conference on Pattern Recognition (ICPR)*, pages 278–283. IEEE, 2018.
- [45] Hong Xuan, Abby Stylianou, Xiaotong Liu, and Robert Pless. Hard negative examples are hard, but useful. In *European Conference on Computer Vision*, pages 126–142. Springer, 2020.
- [46] Hong Xuan, Abby Stylianou, and Robert Pless. Improved embeddings with easy positive triplet mining. In *Proceedings of the IEEE/CVF Winter Conference on Applications of Computer Vision*, pages 2474–2482, 2020.
- [47] Kwang Moo Yi, Eduard Trulls, Vincent Lepetit, and Pascal Fua. Lift: Learned invariant feature transform. In *European conference on computer vision*, pages 467–483. Springer, 2016.
- [48] Baosheng Yu, Tongliang Liu, Mingming Gong, Changxing Ding, and Dacheng Tao. Correcting the triplet selection bias for triplet loss. In *Proceedings of the European Conference on Computer Vision (ECCV)*, pages 71–87, 2018.
- [49] Aihua Zheng, Xianmin Lin, Chenglong Li, Ran He, and Jin Tang. Attributes guided feature learning for vehicle re-identification. *arXiv preprint arXiv:1905.08997*, 2019.
- [50] Liang Zheng, Liyue Shen, Lu Tian, Shengjin Wang, Jingdong Wang, and Qi Tian. Scalable person re-identification: A benchmark. In *Proceedings of the IEEE international conference on computer vision*, pages 1116–1124, 2015.
- [51] Zhedong Zheng, Tao Ruan, Yunchao Wei, Yi Yang, and Tao Mei. Vehiclenet: learning robust visual representation for vehicle re-identification. *IEEE Transactions on Multimedia*, 2020.
- [52] Zhun Zhong, Liang Zheng, Donglin Cao, and Shaozi Li. Re-ranking person re-identification with k-reciprocal encoding. In *Proceedings of the IEEE Conference on Computer Vision and Pattern Recognition*, pages 1318–1327, 2017.
- [53] Yi Zhou and Ling Shao. Aware attentive multi-view inference for vehicle re-identification. In *Proceedings of the*

IEEE conference on computer vision and pattern recognition, pages 6489–6498, 2018.

- [54] Jianqing Zhu, Huanqiang Zeng, Jingchang Huang, Shengcai Liao, Zhen Lei, Canhui Cai, and Lixin Zheng. Vehicle re-identification using quadruple directional deep learning features. *IEEE Transactions on Intelligent Transportation Systems*, 21(1):410–420, 2019.